

AN ABSTRACT OF THE THESIS OF

Christopher Edward Ordonez for the degree of Master of Science in Oceanography
presented on December 14, 2012.

Title: Absolute Water Velocity Profiles from Glider-mounted Acoustic Doppler Current
Profilers.

Abstract approved:

R. Kipp Shearman

This paper details a method to compute absolute water velocity profiles from glider-based acoustic Doppler current profiler (ADCP) measurements based on the “shear method” developed for lowered ADCPs. The instrument is a 614-kHz Teledyne RDI ADCP integrated into the body of a Teledyne Webb Research Slocum Glider. Shear is calculated from velocity measurements and averaged over depth intervals to create a dive-averaged shear profile. Absolute velocities are computed by vertically integrating shear profiles yielding relative velocity profiles and then referencing them to dive-average velocity measurements calculated from glider dead-reckoning and GPS. Bottom-track referenced velocities also provide absolute velocities when bottom-tracking is available, and can be applied to relative velocities, producing absolute velocity profiles through linear fitting. Data quality control is based on ADCP percent good measurements. Compass heading bias corrections are applied to the raw ADCP measurements before averaging shear profiles. Comparison between simultaneous, full-water column velocities referenced to dive-average currents and those referenced to bottom-track profiles, resulted in RMS error values of 0.05 m s^{-1} for both north and east components. During open ocean deployments, the glider ADCP recorded velocities concurrent and proximate to vessel

ADCP measurements in waters of similar thermal characteristics. The combined comparison analysis resulted in RMS error values ranging 0.08-0.31 m s⁻¹ and 0.06-0.21 m s⁻¹ for north and east components, respectively.

©Copyright by Christopher Edward Ordonez

December 14, 2012

All Rights Reserved

Absolute Water Velocity Profiles from Glider-mounted Acoustic Doppler Current
Profilers

by

Christopher Edward Ordonez

A THESIS

submitted to

Oregon State University

in partial fulfillment of
the requirements for the
degree of

Master of Science

Presented December 14, 2012
Commencement June 2013

Masters of Science thesis of Christopher Edward Ordonez presented on December 14,
2012.

APPROVED:

Major Professor, representing Oceanography

Dean of the College of Earth, Ocean, and Atmospheric Sciences

Dean of the Graduate School

I understand that my thesis will become part of the permanent collection of Oregon State University libraries. My signature below authorizes release of my thesis to any reader upon request.

Christopher Edward Ordonez, Author

ACKNOWLEDGEMENTS

I wish to thank my advisor, Kipp Shearman, for taking a chance on me, a seagoing engineer new to the natural sciences. He worked to find my initial funding where there was none readily available. He put me straight to work with leading edge technologies, continually challenged the extents of my analytical skill, and always required my labor to be applied with diligence and quality. He as also been kind, generous, and human to me. Kipp is a decent family man and a serious minded scientist to whom my future professional pursuits are indebted.

I would like to offer my appreciation to the other members and talented scientists of the Oregon State Glider Research Group: Jack Barth, Zen Kurokawa, Anatoli Erofeev, Piero Mazzini, Kate Adams, Alejandra Sanchez, Gonzalo Sauldias Yau, and Pat Welch. Whether working together off the Oregon Coast, putting in extended hours at the lab, piloting the gliders at 4 a.m., supporting each others' work, or sharing dinner & wine, this group has provided support, insight, and community for me.

I would like to thank the Office of Naval Research for funding and supporting the Lateral Mixing Project. This multi-institution research effort provided a large portion of the ocean observations used in this thesis. LatMix also enabled me to participate in three separate deployments into the open ocean over the short course of earning this Masters. I greatly value time spent at sea.

I also wish thank the third member of my Committee, Ed Dever. He has continually provided me with advice and perspective on new ocean observation technologies since I first arrived and has always been welcoming.

CONTRIBUTION OF AUTHORS

Dr. R. Kipp Shearman contributed to the analysis and writing of this thesis. Dr. R. Kipp Shearman, Dr. John A. Barth, Dr. T. Patrick Welch, Dr. Anatoli Erofeev, and Zen Kurokawa contributed to ocean data collection, data processing and sensor analysis. Alejandra Sanchez, Gonzalo Salidias Yau, and Dr. T. Patrick Welch contributed to the surface drift experiment operations. Dr. Stephen Pierce and Craig Risien provided additional data used for comparative analysis.

TABLE OF CONTENTS

	<u>Page</u>
1 INTRODUCTION	1
2 ABSOLUTE WATER VELOCITY PROFILES FROM GLIDER-MOUNTED ACOUSTIC DOPPLER CURRENT PROFILERS	4
2.1 OVERVIEW	5
2.2 Data Sets	9
2.2.1 Glider Deployments	9
2.2.2 Glider Sensor Inputs to ADCP.....	9
2.2.3 ADCP Settings	10
2.2.4 Compass Calibration.....	12
2.2.5 Glider Dive-Average Current Calculations	13
2.2.6 Glider Surface Drift Velocities	16
2.3 Methods.....	18
2.3.1 Data Quality Control.....	18
2.3.2 Depth Interval Averaging and Interpolation	19
2.3.3 Computing Velocities	21
2.4 Results and Discussion	24
2.4.1 Measurement Coverage of Glider Dive	24
2.4.2 Velocity Comparisons in the Coastal Ocean	24
2.4.3 Velocity Comparisons in the Open Ocean.....	27
2.5 Conclusion	30
2.6 Acknowledgments.....	32

TABLE OF CONTENTS (Continued)

3	FURTHER WORK	43
	BIBLIOGRAPHY	47

LIST OF FIGURES

<u>Figure</u>	<u>Page</u>
FIGURE 2.1: ADCP Glider Photographs.	36
FIGURE 2.2: Map of Glider Deployments and Dive-Average Currents.....	37
FIGURE 2.3: Raw velocity measurements vs. depth and all bins for Dive #13 of Oregon Coast deployment.....	37
FIGURE 2.4: Mounting Arrangement Beam Angles of Glider-Mounted ADCP.	38
FIGURE 2.5: Velocity Data and Shear Data Profiles, north direction for Oregon coast dive #13.....	39
FIGURE 2.6: Compass Correction Curve: Glider June with same battery pack before and after Oregon coast deployment.	39
FIGURE 2.7: Regression Plots: Dive-Average Velocities with Biased Headings, Oregon coast dives #2-17.....	40
FIGURE 2.8: Photograph of Glider Drift Test.	40
FIGURE 2.9: North velocity depth interval standard deviation.	41
FIGURE 2.10: Oregon Shelf Dives #2-17, Regression Plots: Dive-Average Referenced vs. Bottom-Referenced Depth Interval Velocities.	41
FIGURE 2.11: Oregon Shelf Dive #13: Velocity Profiles	42
FIGURE 2.12: Cape Hatteras and Glider June Deployment Comparison.	42

LIST OF TABLES

<u>Table</u>	<u>Page</u>
TABLE 2.1: Glider Deployments and Instrument Settings.	33
TABLE 2.2: Velocity Comparison Results.	34
TABLE 2.3: Minimum TWR Slocum variables required to re-calculate dive-average current velocity.	35

1 INTRODUCTION

The integration of Acoustic Doppler Current Profilers (ADCPs) onto Autonomous Underwater Vehicle (AUV) Gliders is a new application of two prolific technologies which offers significant potential for enhancing oceanographic observations. ADCPs determine water velocity by transmitting a sound pulse and measuring the acoustic Doppler shift of the returning signal from scattering material in the water column. When the instrument is within range of the seafloor, over-ground velocities are recorded by bottom-track velocity measurements (RD Instruments, 1996). Gliders are robotic ocean sensor platforms driven by variable negative and positive buoyancy, traveling through the water in a saw-tooth pattern as the pitched glider body and wings translate vertical motion into directed horizontal motion. Glider technology emerged in the 1990's after advances in satellite communication capabilities, accurate GPS positioning, and buoyancy engine technology (Rudnick, et al 2004). Gliders have many integrated oceanographic sensors and development of additional sensors and applications continue (Schofield, et al, 2007). Instruments must be compact to fit on the glider and light weight to allow neutral ballasting. Gliders possess an advantage over other AUVs in their efficient use of energy (Davis, et al, 2003). Glider instruments must have a low power draw to capitalize on the long-duration, ship-free operations. Integrated ADCPs are now becoming available on commercially manufactured gliders due to advancements in instrument compactness and power efficiency.

Whilst making vertical profiles and progressing horizontally, the glider sensors collect concurrent oceanographic measurements. The suite of sensors on a given glider enables researchers to delineate linkages between observed variables. For example, in the

coastal ocean, salinity, and temperature measurements may suggest upwelling currents. Tandem dissolved oxygen measurements allow quantification of the hypoxic effects of the upwelling feature (Grantham, et al, 2004). Likewise, ADCP velocity measurements concurrent to other glider sensor observations can further reveal the dynamic structure of studied ocean locations. Velocity shear and Richardson numbers (Ri) derived from the velocity measurements can provide important values for ocean mixing research.

Glider-based acoustic velocity measurements are currently being applied in various ways. Techniques are being developed to use the Teledyne RD Instruments Explorer Doppler Velocity Log (DVL) to improve glider through-water navigation (Woithe, et al, 2011). High resolution shear measurements have been collected with gliders using the Nortek Aquadopp Profiler (Lohrmann and Nylund, 2008). Dive-average current referenced velocity profiles have been applied with 30-hour smoothing to the coastal ocean (Todd, et al, 2011). The implementation of these methods have many oceanographic research applications. Improved navigation can enhance the acquisition of other sensor measurements by maintaining position on the desired transect. High resolution shear can provide information on plankton thin layer dynamics. Smoothed absolute velocities can confirm or improve geostrophic current calculations.

The research presented in this thesis explores the ability of the glider-mounted ADCP to yield absolute velocity profiles for individual gliders dives consisting of one or more yos. The technology used is a Teledyne RDI Explorer DVL integrated into a Teledyne Webb Research (TWR) Slocum. Over the course of one yo, the instrument can record hundreds of multiple-bin ensembles at different glider depths providing velocity measurement overlap within depth intervals. The research method modifies the “shear

method” developed for Lowered ADCP research, that is depth interval averaging horizontally overlapping velocity bin measurements and referencing relative velocity profiles to dive-average water currents. Effective data filtering, heading bias corrections, and instrument settings to optimize horizontal overlap of measurements are required for this approach. The results of this application are statistically compared to bottom-track referenced velocities measured by the same Explorer DVL and to concurrent, independent ADCP measurements from an observational buoy and research vessels. The agreement between absolute velocities produced from this research and commonly-used independent measurements suggest that application of the modified shear method to glider ADCP measures offer a viable process for use in observational oceanography.

The scope of this thesis focuses on profiles calculated from dive depth interval averaging. Depth interval averaging, however, can be applied to individual yos to yield profiles for vertical shear and bottom-referenced velocities with increased horizontal resolution.

2 ABSOLUTE WATER VELOCITY PROFILES FROM GLIDER-MOUNTED ACOUSTIC DOPPLER CURRENT PROFILERS

Christopher E. Ordonez, R. Kipp Shearman, John A. Barth, T. Patrick Welch, Anatoli Erofeev, Zen Kurokawa

2.1 OVERVIEW

Oceanographic researchers require direct velocity measurements with vertical structure to fully understand the dynamic features of the studied region. Relative velocity observations can produce vertical shear values which yield the Richardson number (Ri) and provide quantitative measures of ocean mixing. Acoustic Doppler technology has been widely utilized by oceanographic researchers to measure water velocity since becoming commercial in the late 1970's (RD Instruments, 1996). A variety of scientific ocean sensor platforms have hosted Acoustic Doppler Current Profilers (ADCPs), each application with differing objectives and strengths. Moored ADCPs provide persistent observations at stationary positions. Ship-mounted ADCPs provide water velocity measurements in the upper ocean with real-time reporting to onboard researchers. Lowered ADCPs (LADCPs) provide velocity profiles over deep ocean water columns by taking horizontally overlapping and consecutive measurements (Fischer and Visbeck, 1993).

Autonomous Underwater Vehicle (AUV) Gliders are now becoming available with incorporated ADCPs enabling current measurements concurrent to other physical and biological sensor measurements from the glider platform (Davis, 2010). Energy-efficient gliders collect high-density measurements for weeks to months without continuous vessel operations and expenditures. The compact size and limited weight of the ADCP unit permits integration inside the glider hull. Sensor weight is an important consideration on a glider as the vehicle must be ballasted neutrally buoyant for operation (Teledyne Webb Research, 2009). Low ADCP power requirements allow long glider

deployments and can be set to record on periodic dive intervals. The integrated ADCP is amongst the expanding suite of sensors available for the gliders (Schofield, et al, 2007).

Data collection and processing methods have been developed to use LADCP to obtain absolute velocity profiles using the “shear method” and the “inverse velocity solution”, (Fischer and Visbeck, 1993, Visbeck, 2002). LADCP systems consist of vertically-oriented ADCPs, mounted onto a Conductivity Temperature Depth (CTD) sensor frame, lowered and raised from vessel winch lines measuring water column velocity relative to the movement of the package. LADCPs can utilize multiple velocity-referencing constraints for each cast, enabling absolute velocity profile calculations. Referencing data includes vessel drift inferred from continuous Global Positioning System (GPS) positions during the LADCP casts, shipboard ADCP measurements in the upper portions of cast, and bottom-track velocity measures where available during the lower cast (Thurnherr, 2010). To obtain absolute velocities the shear method utilizes one reference source and the inverse velocity solution applies multiple references, both for individual casts (Visbeck, 2002).

ADCP operation from a glider shares similar aspects to LADCP deployments that enables application of the depth interval averaging to the measurements, but also has unique constraints requiring different approaches. Gliders use variable buoyancy to descend and ascend in a saw-tooth shaped pattern, collecting water column measurements along the glide path. Gliders have a pitch angle that is effective for vertical sampling and like the LADCP make successive velocity measurements at overlapping depths while descending (Davis, et al, 2003). Gliders have access to GPS only at the surface, before and after dives. The glider uses GPS positioning combined with a dead reckoning

algorithm to calculate dive-average water current velocities (Teledyne WRC 2009, Davis 2002). Dead reckoning calculations use glider attitude, compass heading, and depth changes to model flight vectors. Gliders use GPS to infer water currents during the dive, by calculating the offset between surfacing and dead reckoned positions, whereas LADCP GPS positioning tracks vessel movement during the casts. In both cases, platform motion must be removed to ascertain absolute water velocities. Previous research using the inverse velocity solution and 30-hour Gaussian time-domain filtering has been applied to Spray glider-mounted Sontek 750-kHz ADP measurements to observe water currents (Todd, et al, 2011).

This research utilized two 350-m Slocum Gliders from Teledyne Webb Research (TWR), each integrated with a Teledyne RD Instruments (TRDI) Explorer Doppler Velocity Log (DVL). The Explorer DVL is a 614.4-kHz, 4-beam phased array ADCP depth rated to 1000 m, integrated into a science bay on the glider body and has a compact, downward-facing transducer weighing 1.1 kg. See Fig. 1 for a photograph of ADCP Glider “John.” The two gliders deployed, gliders “June” (unit #186) and “John” (unit #185), are early versions of the Generation 2 Slocum, with oil-filled buoyancy bladder and depth range of 350 m. GPS and Iridium antennae are mounted in the tail, receiving positions and communicating with onshore operators while surfaced. The gliders also include integrated optical fluorometers (WET Labs ECO Triplet and ECO FL) and a CTD (Sea-Bird SBE41). A factory transducer misalignment on Glider John altered its ADCP measurements and reprocessing of the collected data is required. In this paper, only data from Glider June is presented.

Applying the shear method to glider velocity measurements requires data processing, data inaccuracy removal, and post-processing velocity profile comparison. Water velocity measurements from a propeller-driven autonomous platform have been assessed through quantitative comparisons of REMUS AUV-mounted ADCP measurements to concurrent and proximal water velocity profiles from a stationary ADCP (Fong and Jones, 2006). Depth interval averaging velocity requires quality control measures and removal of significant outliers from the collected data (Fischer and Visbeck 1993). Instrument settings should be optimized for long range and high accuracy as best suited to the environmental conditions, (Visbeck 2002). Heading dependent compass errors must be mitigated to correctly calculate dive-average water currents (Gourdea, et al, 2008). Uncertainty in GPS positions will cause errors in surface drift measurements, also affecting dive-average water current values (Merckelbach, et al, 2008).

The objective of this study is to obtain absolute velocity profiles from glider-based ADCPs for dives (consisting of multiple yos) by modifying the shear method. The accuracy of the absolute velocity profiles are tested by comparison to bottom-tracked velocity measurements and nearby moored and ship-based ADCP measurements. Section 2 describes the data sets collected, Section 3 details the implementation of the LADCP shear method for glider-based ADCPs, Section 4 discusses the resulting absolute velocity estimates and the comparison to other measurements.

2.2 Data Sets

2.2.1 Glider Deployments

Data for this analysis were collected by ADCP-gliders in coastal and deep-ocean locations with differing environmental conditions affecting ADCP performance. In September 2011, Glider June flew along the Newport Hydrographic Line (NH Line) which occupies the 44.65° N latitude westward of the 25-m isobath on the Oregon shelf. The glider transects are predominantly cross-shelf. These coastal waters contains abundant scatterers, allowing higher resolution settings. Dives #2-17 are used for comparative analysis where bottom-track is available for the full water column. Dive #1 was a test dive, and dives #18 and onward did not have bottom-track for the full profile depth. In June 2011, the ADCP gliders were deployed in the Sargasso Sea which contains few scatters in the water column and has a seafloor too deep for the ADCP to collect of bottom-track velocity measurements. In February/March 2012, both gliders were deployed in the North Atlantic Gulf Stream region where bottom-track measurements were also unavailable. See Fig. 2 for a map of glider deployment locations and Table 1 for glider deployment and instrument settings.

2.2.2 Glider Sensor Inputs to ADCP

The ADCP records raw water velocity, bottom-track velocity, and data quality information for each bin of each ensemble (Teledyne RD Instruments, 2010). Unlike typical models, this ADCP receives heading, pitch, roll, and depth data from the glider's sensors, for each ensemble. The ADCP measures velocities in beam coordinates relative to the transducer and converts the data to glider and earth coordinates based on data from

glider pitch, roll, and compass sensors. Post-mission analysis assigns depths to each bin based on glider depth, pitch, roll, bin size, bin number, and blanking distance.

Dive profiles can encompass long horizontal distances relative to the vertical range. In one common six-hour dive traveling 0.35 m s^{-1} horizontally, the glider can transit approximately 7.6 km absent water current influence (Rudnick, et al 2004). Each dive consists of one or more yos (a glider descent/ascent cycle), with four yos being a common number per dive. The horizontal yo distance traveled with a 26-deg pitched descent/ascent is approximately four times the vertical distance. Velocity measurements are only recorded during the descent of the yo. Each ADCP ensemble of the yo is recorded from a successively deeper position with an ADCP range that often varies with depth. The result is a diagonal swath of variable thickness, where velocity measurements overlap at each depth. Multiple yos in the dive increase the overlapping velocity values at each depth. See Fig. 3 for a plot of raw velocity measurements versus depth and yo ensemble for Dive #13 of the Oregon coast deployment.

2.2.3 ADCP Settings

The multi-element phased-array transducer face is tilted forward by 11 degrees to optimize three-beam measurements on the 26 degree pitched glider descents. This configuration allows the three forward ADCP beams to orient 15 deg from vertical on descents while the fourth is 45 deg aft relative to the glider, see Fig. 4. The transducer angle is fixed forward, making the instrument orientation unsuitable for collecting measurements during ascents. While the instrument is oriented to record on the descent, data collection often starts before the glider has fully achieved its dive angle resulting in inaccurate measurements.

The ADCP uses attitude and compass data from the glider sensors for orientation. This is required for converting beam-relative velocities into earth-coordinate velocities and for dead-reckoning calculations. All water velocity data used in this research were collected in earth-coordinates and converted from magnetic to true north orientation. Magnetic declinations were calculated from the midpoint between latitude and longitude extents for each deployment using a National Geophysical Data Center (NGDC) algorithm (National Geophysical Data Center, 2012).

Similar to LADCP deployments, glider mounted ADCP settings should be optimized for data density and signal range to produce more precise shear and velocity depth interval averages from ensemble data (Fischer and Visbeck, 1993). ADCP bin measurements begin below a blanking distance (0.88 m) to avoid data noise from transducer ringing. As the glider descends and collects data, subsequent ensemble velocities overlap at the same water depth intervals. Greater signal range of acceptable velocity returns and faster ping rates will increase measurement density within each depth interval. The maximum range is set by the user with the bin number and bin size parameters, but range is ultimately limited by environment conditions. Water columns with fewer scatterers will limit the range. Setting the ADCP to transmit narrow bandwidth pings instead of wide extends the depth range, but decreases single-bin precision. Designating larger bin sizes can extend the range while reducing vertical resolution (Teledyne RD Instruments, 2010).

In high-scattering, coastal Oregon waters, ADCP settings were 2-m bin lengths, 30 bins per ensemble, and wideband transmission. The ADCP collected bottom-track

velocities when altitudes were 65-75m. Common coastal ranges were 0-16 bins (0-32 m) in the 0-150 m depth range and 3-10 bins (6-30 m) at 150-300 m depths.

In the low-scattering and deep North Atlantic Ocean locations, ADCP settings were 4-m bin lengths, 30 bins per ensemble, and narrowband transmission. Because ocean depths exceeded the ADCP range, bottom-tracked velocities were not obtained. Common ranges for measured velocities were 3-7 bins (12-28 m) for 0-150 m glider depths and 0-3 bins (0-12 m) at 150-350 m depths.

For all locations the time-between-pings were set to fast-as-possible and pings-per-ensemble were set to 10. The average time-per-ensemble was 3.4 sec. for Oregon, 4.2 sec. for the Sargasso Sea, and 3.4 sec. for the Gulf Stream deployment, excluding outliers greater than 30 sec. The glider has an approximate descending vertical velocity of 0.10 m s^{-1} . During the 3.4 seconds of one ensemble, the glider travels a vertical distance of 0.34 m, which is less than the 2 m and 4 m bin size settings. See Table 1 for instrument settings.

For all velocities and shear values of each dive, we calculate a depth based on glider depth, bin length, bin number, and glider pitch. Oregon deployment dive #13 velocity and shear data is displayed in Fig. 5 with depth versus magnitude after the depth-assigning calculation is applied. After depths are established, the data is averaged within discrete depth intervals to produce single velocity and shear profiles for the dive.

2.2.4 Compass Calibration

In order to correctly establish earth-referenced velocity components, accurate vehicle heading is required. Glider compasses have observed heading-dependent biases influenced by the magnetic properties of the glider body, internal hardware, and from the

exchangeable battery packs (Gourdeau, et al 2008, Merckelbach, et al 2008). Glider compass biases can vary for different battery packs, and manufacture-supplied calibration software does not fully remove these biases from the recorded heading values. True and measured heading differ by as much as ± 25 deg with the offset magnitude being a sinusoidal function of compass heading; see Fig. 6. Over the course of a deployment, heading biases from the same battery pack have also been found to change. During the nine day Oregon coast deployment the heading bias amplitude changed from 10.4 to 7.1 deg. Directional biases must be established by positioning the glider on a true compass rose and measuring reported headings. Heading correction values will be a function of the recorded glider heading and the bias. The heading corrections to water and bottom-track velocity components are applied to each ensemble. Components are recalculated from the corrected heading and the magnitude. Heading bias measurements found in this research were obtained either pre- or post-mission, resulting in a single correction that was applied to the full mission data set.

2.2.5 Glider Dive-Average Current Calculations

Dive-average water velocities are calculated by differencing anticipated surfacing positions calculated from internal glider flight-model dead-reckoning to those actual GPS-reported surfacing positions (Rudnick, et al 2004). Dive-average current calculations rely on headings from the glider compass which require recalculation with corrected headings. The glider calculates one horizontal water current velocity vector per dive. The glider's dead-reckoning calculation uses glider attitude, vertical velocity (derived from pressure and time), and glider operational-state variables to infer horizontal glider travel distance. The water currents which cause the difference between the

calculated and actual surfacing positions may vary temporally and spatially during the dive. The resulting dive-average water current calculation will not reflect whether these encountered currents were constant or variable.

The glider calculates through water dead reckoned positions using a proprietary algorithm to establish glider speeds and positions while flying underwater and unable to collect GPS signals (Lauren Cooney TWR, personal communication, October 2012). This research recreates the dead reckoning calculation using the corrected heading, glider attitude, and glider operational-state variables, though it is not exactly the same calculation as the one performed by TWR software.

The dive-average current calculation summary is as follows:

1. Identify initial position from GPS fix before glider dive, \vec{x}_0 .
2. Calculate vertical speed from change in pressure over change in time, $\frac{dp}{dt}$.
3. Calculate the horizontal_speed $|u|$, from vertical speed, pitch θ , and angle of attack α .

$$|u| = \frac{dp}{dt} * \cos(\theta + \alpha) \quad (1)$$

4. Calculate horizontal velocity vector \vec{u} with corrected heading.

$$\vec{u} = |u| * \cos(\text{heading} - 90) + i * \sin(\text{heading} - 90) \quad (2)$$

5. Integrate velocity to obtain dead reckoned surfacing position, \vec{x}_{DR} .

$$\vec{x}_{DR} = \int_0^T \vec{u} * dt + \vec{x}_0 \quad (3)$$

6. Obtain glider surfacing position \vec{x}_{GPS} from extrapolation of surface drift.

7. Calculate dive-average current vector \vec{V}_{DA} from position difference and time of dive.

$$\frac{(\vec{x}_{DR} - \vec{x}_{GPS})}{\Delta T} = \vec{V}_{DA} \quad (4)$$

For each deployment the algorithm used in this research is analyzed against the glider calculated values, both using uncorrected heading measurements. Comparisons show significant correlation, but slopes suggest our calculation may produce dive-average currents that differ from the TWR values by scaling factor. For the Oregon coast deployment regression analysis resulted in the following: slope: 1.15 ± 0.07 , offset: $0.00 \pm 0.04 \text{ m s}^{-1}$, and R^2 : 0.97 for north (V) dive-average velocity, slope: 1.04 ± 0.16 , offset $0.00 \pm 0.02 \text{ m s}^{-1}$, and R^2 : 0.82 for east (U). RMS errors were 0.01 m s^{-1} and 0.03 m s^{-1} for north (V) and east (U), respectively. See Fig. 7, for regression analysis plots. Scaling factors are calculated from the inverse slope of biased heading water current regression. Scaling factors are then applied to corrected heading water current calculations for velocity referencing. For the Oregon Coast deployment, water current calculations are scaled by 0.87 for V and 0.96 for U velocity components.

Because water current calculations use the same variables as TWR algorithms, except for heading, resulting values are susceptible to the same biases. See Table 3 for glider variables required for re-calculating dive-average currents. For example, experiments using the Spray glider have found that the length of time during the dive when the glider vertical motion is slower (e.g. during lower portions of the down-yo) will bias the dive-average water current calculation to water currents present during those instances (Gourdeau, et al, 2008). Glider dive-average current calculations include motion from the upcasts for which there is no ADCP data. Dive-average referenced

velocities are calculated for each profile by finding the relative velocity profile mean, subtracting that value from the dive-average water current, and adding the remainder to the relative profile. Because the ADCP measurements are not collected on the upcast, but water current measurements are, upcast current biases will be included in the referencing.

2.2.6 Glider Surface Drift Velocities

Surface currents can be calculated from glider drift between dives and provide an independent check on absolute velocity profiles. After completing a multi-yo dive, the glider calls via Iridium satellite phone to send data files and receive pilot instructions. During the 10-20 min. interval at surface, the glider collects GPS fixes and drifts with surface currents. Surface currents can be estimated based on the change in glider position over time at the surface. The average of surface currents between two successive surfacings should roughly match the upper profile velocities of the absolute velocity profiles collected during the dive. Wind driven currents, however, will likely be faster at the surface (Marshall and Plumb, 2008)

GPS fixes received immediately after surfacing or closely preceding a dive can be inaccurate and inappropriate for velocity calculations. GPS data used for the drift calculation are filtered to have uncertainty values less than 2 m. Drifts further than 10 km or with durations longer than 12 hrs were removed because these values indicate a disruption to the operation, such as interim glider recovery to the vessel.

The glider body is not designed to be a Lagrangian float, but its drift characteristics are indicative of surface currents. We performed an at-sea experiment measuring the spatial separation of an ADCP glider drifting concurrent to two CODE-style floats for eight 30-min drifts (Davis, 1985). We compared speed over ground (SOG)

because the drift directions were similar for all items. CODE Float SOG drifts deviated from each other by less than 2%. Regression analysis of the drift SOG comparisons between glider and floats yielded a slope of 0.83, offset of 0.09 m s^{-1} , and R^2 of 0.87. RMS error between SOG drifts was 0.01 m s^{-1} over a SOG range of $0.55\text{-}0.65 \text{ m s}^{-1}$. This experiment suggests that the glider drift is an approximate Lagrangian float and surface drift velocity calculations may agree with surface currents. During this research, surface drift velocities were compared to upper-profile, absolute velocities from the ADCP. Given the current limitations of surface drift velocity characterization, the comparisons were used only to aid in method development, check order of magnitudes and temporal trends. Further drift experiments would help to increase the accuracy of the glider drift characterization. See Fig. 8 for image of glider drift experiment.

2.3 Methods

The objective of this method is to produce absolute horizontal velocity profiles over the full depth of each dive from limited-range, relative-to-glider ensemble ADCP data. Raw velocity measurements include absolute water velocities, platform velocities, and noise. The gliders in this experiment do not have accelerometers, positioning beacons, or other means of obtaining accurate glider positions and velocities while submerged and out of acoustic range from the seafloor. Taking the vertical central difference of raw water velocities for each ensemble provides the shear values for each bin (Fischer and Visbeck, 1993). See Fig. 5b. Depth interval averaging shear values creates a shear profile. Integrating the shear profile yields a velocity relative to the bottom dive-depth, independent from glider motion. Referencing the relative velocity then produces absolute velocity (Thurnherr, 2010).

2.3.1 Data Quality Control

The ADCP is mounted with an orientation to collect water velocity data during the descent, but the instrument often starts recording before the glider has completed its apogee maneuver and pitched to -26 deg. Velocities collected before the glider achieves half the descent angle (-13 deg.) or while it is still changing pitch per ensemble at magnitudes greater than 1 deg are removed. The glider spends 94%-96% of its descent duration pitched steeper than -13 deg., but other factors influence the time and depth of the descent measured by the ADCP, including scatterer density and the glider's automated ADCP off-switch at the descent bottom. The pitch change filter is applied to a pitch curve smoothed with a three point moving average to avoid fluctuating pitch angles

activating the filter deeper than desired. Raw water and bottom-track velocities with a percent good value less than 90% are removed. Velocities from locations within 3 m of the seafloor are removed to avoid acoustic sidelobe contamination (RD Instruments, 1996). Bottom-track velocities have an observed range of 65-75 m altitude and the operational manual specifies a bottom-tracking range of 100 m (Teledyne RDI, 2010). Values near the upper range can be sparse and contain increased, consequently velocities recorded at above 70 m altitude are removed when bottom range values are available from the instrument. Locally weighted scatter plot smoothing (i.e. “Lowess” smoothing) is also applied to bottom-track values and resulting values deviating greater than two standard deviations from mean are removed. Ensembles recorded with the glider roll angle is greater than 18 deg are removed according to LADCP conventions, but such roll is rare in glider data. Data filtering is necessary to creating accurate profiles, (Fischer and Visbeck, 1993).

2.3.2 Depth Interval Averaging and Interpolation

Depth interval averaging takes successive, horizontally overlapping shear bin data, turning ensemble measurements limited to the transducer range, into a profile over the full dive-depth (Visbeck, 2002). Data density for the depth intervals is a function of ensemble vertical range, time per ensemble, accuracy of raw water velocities, and number yos per dive. The density is also dependent on the depth interval length, which is 2 m for this research. When the glider is pitched for descent the transducer face is not horizontal and bin length does not represent the true vertical distance of velocity measurements. The bin depth (D_{Bin}) calculation must include this correction as follows (Gregory Rivalan TRDI, personal correspondence, November 2012):

$$D_{Bin} = D_{Glider} + Blanking_Dist. + Bin_Size * Bin_Num. - \frac{Bin_Size}{2} * \cos(11^\circ + Pitch) \quad (5)$$

The data density of profile depth intervals are a geometric function of the factors mentioned above, but in practice, the number of averaged bin values vary due to changing signal depth ranges and percent good data filtering. At depth intervals where the data density is low, noisy velocity values (and resulting shear) can disproportionately influence the average and produce inaccurate values. Noise and low data density may result from sparse scatterers. Low data density also occurs near the beginning and end of yos due to fewer overlapping ensembles per depth interval. Setting a minimum number of data points required for depth interval averaging reduces erroneous profile values. We set the minimum number of data points to 15 for the upper and lower 10 bins of each profile in order to target area where erroneous averages proliferate and decrease frequent mid-profile gaps.

Mid-profile gaps may occasionally result from lack of measurements. Where mid-profile data gaps occur, shear values were calculated by interpolating values from adjacent depth intervals to avoid creation of erroneous velocity profiles by including data gaps while integrating vertical shear profiles. The average profile percentage of interpolated depth interval gaps were 0.9%, 0.2%, 1.8%, and 0% for all Oregon dives, Oregon nearshore dives, Sargasso Sea, and Gulf Stream deployments, respectively. Isolated shear values may remain at depths far from the grouping of continuous depth interval values. Shear depth interval values below data gaps of 20 intervals or more, are removed. Interpolating between these large gaps would otherwise create erroneous values.

2.3.3 Computing Velocities

Once the shear profile is established, the values are trapezoidally integrated starting from the deepest depth interval of the dive to create a velocity profile relative to the dive-bottom. Velocities collected from the lower depths consistently have lower depth interval standard deviation. Standard deviation calculations of raw velocity depth intervals generally show values (approx. $0.15\text{-}0.2\text{ m s}^{-1}$) above the baseline (approx. 0.05 m s^{-1}) in the upper water column (approx $5\text{-}20\text{ m}$ depth) and increased for water columns shallower than 50 m ; see Fig 9. for plot of north velocity depth interval standard deviation from the Gulf Stream deployment. For depth intervals above the upper extent of shear profile data, no velocities are calculated to avoid creating values where data was not collected.

Referencing combines relative velocity data with an additional data source to obtain absolute velocity. Referencing an integrated relative velocity profile to dive-average water current velocity yields an absolute velocity profile for the vertical extent of dive. Referencing adds the dive-average current and subtracts the relative velocity profile vertical mean from the relative velocity depth interval velocities. For example, if the dive-average was 0 m s^{-1} , the absolute velocity profile would need to average to 0 m s^{-1} .

$$\begin{aligned} \text{Absolute_Velocity} = & \text{Relative_Velocity (n depth intervals)} + \\ & \text{Dive_Averaged_Current} - \text{Vertical Mean Relative Velocity} \end{aligned} \quad (6)$$

For the calculation of vertical mean relative velocity, the deepest velocity value is repeated for depth intervals near the bottom of the glider path, that otherwise have no velocity data. Similarly, the upper depth interval velocity is repeated in depth intervals extended up to the shallowest glider depth. The mean is then computed for all depth

intervals. This method will produce a mean that better reflects the currents influencing the dive-average current calculation and increases referencing accuracy.

Dive-average referencing is suitable for dives, not for individual yos, because the dive-average values are influenced by the entire dive. Current variability may increase during longer duration dives, but the glider only calculates one averaged current for the entire dive. Integrated velocities referenced to dive-average water velocities are here termed “dive-average referenced velocities.”

Bottom-track measurements are based off pings returning from the seafloor and provide a speed of the instrument over ground. Referencing bottom-track to raw water velocities yields absolute water velocities, here “bottom-referenced velocities.” Bottom-referenced velocity profiles are created using the depth interval averaging strategy at 2 m interval lengths. The same minimum depth interval data point criteria is applied to the upper and lower intervals of bottom-referenced profiles.

If quality control measures do not adequately filter inaccurate velocity measurements, shear profiles can propagate errors when integrating into relative velocity profiles which may result in diverging trends compared with the profile of bottom-referenced velocities, (Visbeck 2002). The diverging profiles can have vertical structure that are not constant with depth, vary in magnitude, and trend differently for each dive. Relative velocity profiles can diverge, either positively or negatively, during integration.

A strategy to lessen the divergence of velocity profiles and further utilize bottom-referenced velocity data, fits integrated profiles to bottom-referenced velocities where available. Linear regression is applied to the difference of integrated and bottom-referenced velocity profiles, establishing a divergence trend and offset. Differences

greater than two standard deviations are not included in the regression. The resulting linear trend and constant offset are then removed from integrated profile producing an absolute velocity, here “bottom-fitted” velocity. The calculation is performed for all profiles where any bottom-track velocities are present. Even if the diverging trend is not removed from the integrated velocity profile, the relative velocities will still be referenced to bottom-track values and become an absolute velocity profile.

2.4 Results and Discussion

2.4.1 Measurement Coverage of Glider Dive

The velocity profile vertical extents can differ from the depths of the glider dive. Data quality filtering and backscatter contribute this difference. The deployment averages of the difference between the top depth of the velocity profile and the top of the glider dive (generally, 0 m) and were 5.1m, 22.4 m, and 10.3 m, for the Oregon nearshore, Sargasso Sea, and Gulf Stream deployments, respectively. The differences between the bottom depth of the glider dives and the bottom of the velocity profiles were dependent on scatterer availability. The Oregon nearshore deployment average difference between glider dive maximum depth and the velocity profile was -1.0 m, indicating that the ADCP range extended passed the glider dive range. Seven of the sixteen dives featured velocity profiles below the dive bottom. The Gulf Stream deployment bottom difference was -11.8 m, with every velocity profile extending below the dive bottom depth. The Sargasso Sea deployment velocity profile depth ranged between 60 m and 160m with a distribution independent of glider dive depth. Excluding the first 12 dives in which the glider dove to 350 m, the remaining 70 dives had an average difference between glider dive maximum depth and the velocity profile of 35.2 m where the glider dove between 120 m and 160m. The limited ADCP range suggests that the Sargasso Sea deployment area contained few scatterers at depth.

2.4.2 Velocity Comparisons in the Coastal Ocean

The glider deployment on Oregon shelf transited through shallow water during the first transect and in proximity to an observational buoy equipped with an ADCP. Both

aspects allow for comparative analysis of the dive-referenced velocity profiles. Velocity profiles calculated from glider dives 2-17 included bottom-track measurements for the full profile depths. Comparing dive-average referenced velocity and full-depth bottom-referenced velocity profiles provides a comparison that takes into account the full scope of profile error and variance, thus providing a more comprehensive analysis.

Linear regression analysis for north (V) velocities between corresponding dive-referenced and bottom-referenced depth interval values yielded a slope = 1.01 ± 0.08 , y-intercept = $0.03 \pm 0.01 \text{ m s}^{-1}$, and $R^2 = 0.63$, where bottom-referenced velocities are the x-axis. See Fig. 10 for regression plots. RMS error calculation yielded 0.05 m s^{-1} . For east (U) velocities the same analysis produced a slope = 1.13 ± 0.15 , y-intercept = $0.02 \pm 0.01 \text{ m s}^{-1}$, $R^2 = 0.39$, and RMS error = 0.05 m s^{-1} . Coincident velocity profiles show broad vertical structure agreement.

The glider made an east-west oriented dive north of the Newport Hydrographic Line Observation Buoy (NH10 Buoy). The average distance of the glider to buoy during this Dive #13 was 3.76 km northward and 0.96 km eastward. The dominant velocity characteristics in this eastern boundary coastal environment are alongshore currents, which are meridional at this transect, increasing the potential that the buoy and glider ADCP observe the same water (Huyer, 1990). The Dive #13 average temperature measured by the glider above 10 m was 12.24 C. The buoy measured temperature at approximately 2.5 m depth using the TRDI Sentinel Workhorse 300-kHz ADCP temperature sensor. The averaged buoy temperature over the glider dive time extents was 12.11 C, suggesting the surface waters may have similar thermal signatures. The buoy is

in 83 m water depth and glider ADCP bottom-referenced velocities were available from 6 m depth for 77 m of the water column.

Dive #13 had a distance of 2.00 km between end points and duration of 2.65 hrs. For comparison, NH10 bin velocities were averaged at each depth interval to produce a velocity profile during the same time interval. Glider depth interval velocities in 2 m bins were interpolated to match the 2m NH10 bins which coincided with different depths. Linear regression analysis between the north (V) velocities of the NH10 averaged profile and the glider dive-average referenced profile resulted in a slope = 1.26 ± 0.60 , y-intercept = $0.03 \pm 0.05 \text{ m s}^{-1}$, and $R^2 = 0.41$, where NH10 velocities are the x-axis. RMS error was 0.05 m s^{-1} . East (U) velocity comparison resulted in slope = 1.12 ± 0.48 , y-intercept = $0.03 \pm 0.02 \text{ m s}^{-1}$, $R^2 = 0.46$, and RMS error = 0.04 m s^{-1} . See Fig. 11 for Dive #13 velocity profiles.

Qualitative comparison between dive-average referenced velocity and NH10 velocity suggests that the north component matches the dive-average velocity profile structure and differs by a constant $\sim 0.05 \text{ m s}^{-1}$. Bottom-referenced north velocities more closely matched the NH10 profile. The north component of the surface current, averaged from the surface drift calculation before and after Dive #13, was 0.005 m s^{-1} , closest to the NH10 profile upper bin velocity. These aspects suggest that the dive-average profile for Dive #13 may be referenced to a velocity over-correcting by a value approximately consistent with the RMS error. Qualitatively, the buoy-measured east component matches profile structure with the dive-average velocity, increasing positive separation from near 0 m s^{-1} at the bottom to 0.08 m s^{-1} at the top of profile. The bottom-referenced profile shows increasing negative separation. The surface current average for the dive is 0.14 m

s^{-1} which most closely matched the dive-average velocity top bin. The NH10 profile has a structure with features not represented in either dive-average referenced or bottom-referenced velocities, suggesting possible different velocity features present between the glider and buoy.

Bottom-referenced velocities from the glider compared to the buoy ADCP measurements with RMS errors of 0.02 m s^{-1} and 0.03 m s^{-1} for V and U, respectively. Linear regressions comparisons yielded a slope = 0.75 ± 0.30 and y-intercept = $0.02 \pm 0.03 \text{ m s}^{-1}$ for the north (V) and a slope = 0.83 ± 0.46 and a y-intercept = $-0.02 \pm 0.02 \text{ m s}^{-1}$ for the east (U) components. The low RMS error values provide indication that the ADCPs measured similar water masses. Bottom-fitted velocity profile structures, north velocities (V) appear to align with the buoy ADCP measurements more closely than the dive-average referenced velocities based on the plots. See Fig. 6 for velocity profile comparisons. The results of the regression comparison between bottom-fitted velocities and the buoy did not statistically improve against the dive-average current referenced velocity results. See Table 2 for comparison details.

2.4.3 Velocity Comparisons in the Open Ocean

During the June 2011 deployment in the Sargasso Sea and March 2011 deployment in the North Atlantic Gulf Stream, Glider June's flight path had close spatial-temporal ranges to research vessel positions that allowed for comparative analysis of ADCP measurements. Only three deployments met the criteria for analysis. During the 2011 deployment, the vessels and gliders followed a NNW-traveling large-scale thermal filament concurrently for approx. 280 km along-stream and had two suitable vessel ADCP data sets for comparison. During the 2012 Gulf Stream deployments gliders and

vessels followed a path approx. 370 km along-stream had one suitable vessel ADCP data set. See Fig. 2 for glider deployment maps and dive-average current velocities. For each of the experiments the vessels generally made cross-stream transects through the thermal ocean feature, whereas the glider flight paths were generally along-stream.

Vessel ADCP measurements were compared to individual glider dive profiles. To isolate the vessel ADCP measurements for each glider dive, only data collected during the time extents of the dive and within 1 km of the straight line between glider diving and surfacing locations. Corresponding velocity bins of vessel ADCP measurements were averaged to create one vessel velocity profile to compare to the one glider velocity profile for the dive. To further ensure measurement of the same water mass, only dives were considered in which the average surface temperature recorded by the vessel and the glider-recorded upper 10m temperature average differed by less than 1 °C. The thermal filter criteria did not remove any compared profiles from the two 2011 data sets, but did remove 3 of the 12 profiles from the 2012 Gulf Stream data set otherwise meeting the spatial-temporal proximity filter. Large temperature gradients are associated with velocity differences in the Gulf Stream North Wall region.

Two vessel ADCP data sets met the criteria for the 2011 deployment. Measurements from the R/V Cape Hatteras TRDI 300-kHz Workhorse ADCP provided 15 comparative profiles. The R/V Oceanus collected data with a TRDI 75-kHz Ocean Observer ADCP, provided 10 velocity profiles. Overlapping vessel and glider data ranges enabled comparisons from 20 m to 130 m depth. Regression analysis of the glider dive-average referenced velocities to the Cape Hatteras showed the closest correlation and smallest RMS errors of all three of the open ocean data set comparisons. See Fig. 12 east

(U) component regression plot and averaged velocity profiles including all concurrent velocity measurements. North velocity linear regression resulted in a slope of 1.05 ± 0.06 , offset of $-0.08 \pm 0.07 \text{ m s}^{-1}$, and R^2 of 0.88. East velocity linear regression produced slope of 0.85 ± 0.06 , offset of $0.00 \pm 0.04 \text{ m s}^{-1}$ and an R^2 of 0.87. RMS errors were 0.08 m s^{-1} and 0.06 m s^{-1} , north and east velocities, respectively. Comparison to Oceanus ADCP data showed RMS errors of 0.10 m s^{-1} and 0.08 m s^{-1} , north and east velocities. See Table 2 for comparison details.

Gulf Stream vessel ADCP data during 2012 from the R/V Knorr provided a greater range of velocities for comparison. Vessel and glider data ranges coincided from 10 m to 146 m depth. Vessel ADCP data during 2011 ranged from approximately -0.05 to 0.6 m s^{-1} and -0.45 to 0.05 m s^{-1} for north and east velocities. Knorr measurements ranged from approximately -0.1 to 1.6 m s^{-1} for north and east. Knorr to glider RMS error values were 0.31 m s^{-1} and 0.21 m s^{-1} , north and east.

2.5 Conclusion

Glider-mounted ADCPs offer a mobile platform for collecting high-resolution water velocity profiles from dense data measurements but require attentive data processing to address the multiple sources of possible error. The resulting velocity RMS errors found in this analyses ranged 0.040-0.31 m s⁻¹.

Shear and absolute velocity profiles are developed for each dive by applying the shear method to instrument-relative velocity measurements and appropriately referencing to glider dive-average water currents. Absolute velocities are also attained by referencing raw water velocities to bottom-track measurements where available. Bottom-fitted velocities, employs bottom-track referencing up though the water column to attain absolute velocities.

Implementing quality control to the data is necessary to achieve accurate shear and dive-average referenced velocity profiles. Instrument settings should increase depth range, utilize bottom-referenced velocities where possible, and increase horizontal velocity data overlap. Processing methods need to address the fact that dive-average water current calculations are influenced by the total glider dive whereas the glider ADCP collects usable measurements on the descents, between apogee maneuvers. Compass bias corrections are critical for accurately obtaining earth-coordinate velocities and revising dead-reckoning calculations. Recalculating dive-average currents with corrected headings using a simplified algorithm creates a potential source of errors. A deployment-specific scaling factor is established based on the linear regression slope comparing our dive-average current calculation and the TWR calculation each with biased headings. The scaling factor is then applied to our dive-average current calculation

with corrected headings, in order to reduce errors from incorrectly estimating glider through-water speed.

The process required to achieve absolute velocities is data and calculation intensive, drawing on many sensors and recorded glider variables. Reducing errors based on correct assumptions in every aspect of the data processing is requisite to implementing the shear method with dive-average referencing constraints. The benefits to oceanographic research of producing high-resolution shear and absolute velocity profiles from glider platforms will be significant where traditional ADCP observations are logistically or economically prohibitive, where multiple mobile platforms are required, and in innovative applications as glider capabilities and uses advance.

2.6 Acknowledgments

NSF grants OCE-0527168 and OCE-0961999 provide principal support for the OSU Glider Research Group, the Oregon ADCP test, and continual NH Line data collection. OSU participation in the Lateral Mixing Project is under the ONR award, N00014-09-1-0379. Thanks to Jerry Mullison and Matt Burdyny of Teledyne RD Instruments, and to Chris DeCollibus and Lauren Cooney of Teledyne Webb Research for detailed technical support. Thanks to Steve Pierce (OSU) for Lateral Mixing vessel ADCP data and technical advice. Thanks to Murray Levine, Craig Risien, and David Langner (OSU) for the NH-10 mooring data, funded by the NSF cooperative agreement Coastal Margin Observation& Prediction (CMOP) (OCE-0424602) and by the National Oceanic and Atmospheric Administration (NOAA) through the Northwest Association of Networked Ocean Observing Systems (NANOOS), grant NA08NO54730290.

Deployment	DVL Settings	Environmental Conditions	Start Date	Mean Coordinate
LatMix 2011 Sargasso Sea Glider June	Bin Size: 2 m Band: Broad Pings/Ensemble: 10 Avg. Ensemble Interval: 4.17 sec. Profile Depth Interval: 2 m	Deep Open. Few Scatterers.	13-Jun-2011	33.221 N, 73.678 W
Oregon Coast Glider June	Bin Size: 4 m Band: Broad Pings/Ensemble: 10 Avg. Ensemble Interval: 3.40 sec. Profile Depth Interval: 2 m	Coastal Shelf. Sufficient scatterers.	19-Sep-2011	44.679 N, 124.457 W
LatMix 2012 Gulf Stream Glider June	Bin Size: 4 m Band: Narrow Pings/Ensemble: 10 Avg. Ensemble Interval: 3.37 sec. Profile Depth Interval: 2 m	Deep Open. Gulf stream influence.	01-Mar- 2012	38.687 N, 64.853 W

TABLE 2.1: Glider Deployments and Instrument Settings.

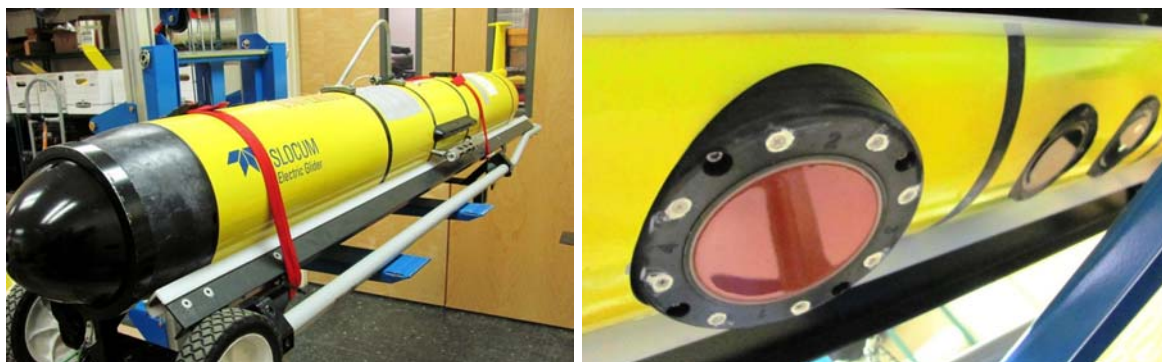
Glider	BR, Oregon	NH10 Buoy	Cape Hatteras Sargasso Sea	Oceanus Sargasso Sea	Knorr Gulf Stream
DAR (V)	M: 1.01 \pm 0.08 C: 0.03 \pm 0.01 R ² : 0.63 RMS: 0.05	M: 1.26 \pm 0.60 C: 0.03 \pm 0.05 R ² : 0.41 RMS: 0.05	M: 1.05 \pm 0.06 C: -0.08 \pm 0.07 R ² : 0.88 RMS: 0.08	M: 1.08 \pm 0.28 C: -0.11 \pm 0.17 R ² : 0.38 RMS: 0.10	M: 0.96 \pm 0.06 C: -0.25 \pm 0.12 R ² : 0.84 RMS: 0.31
DAR (U)	M: 1.13 \pm 0.15 C: 0.02 \pm 0.01 R ² : 0.39 RMS: 0.05	M: 1.12 \pm 0.48 C: 0.03 \pm 0.02 R ² : 0.46 RMS: 0.04	M: 0.85 \pm 0.06 C: 0.00 \pm 0.04 R ² : 0.87 RMS: 0.06	M: 1.23 \pm 0.26 C: 0.10 \pm 0.09 R ² : 0.47 RMS: 0.08	M: 0.85 \pm 0.15 C: 0.23 \pm 0.42 R ² : 0.40 RMS: 0.21
BR (V)	N/A	M: 0.75 \pm 0.30 C: 0.02 \pm 0.03 R ² : 0.49 RMS: 0.02	N/A	N/A	N/A
BR (U)	N/A	M: 0.83 \pm 0.46 C: -0.02 \pm 0.02 R ² : 0.34 RMS: 0.03	N/A	N/A	N/A
BF (V)	Not Independent	M: 1.25 \pm 0.53 C: 0.01 \pm 0.05 R ² : 0.47 RMS: 0.03	N/A	N/A	N/A
BF (U)	Not Independent	M: 0.59 \pm 0.25 C: -0.01 \pm 0.01 R ² : 0.47 RMS: 0.03	N/A	N/A	N/A

TABLE 2.2: Velocity Comparison Results.

DAR: Dive-Average Referenced Velocity. BR: Bottom-Referenced Velocity. BF: Bottom Fitted Velocity. LM11/12: Lateral Mixing Project 2011 / 2012. M = Linear regression slope where variable from the header row is the x-axis. C: Linear regression y-axis intercept (m s^{-1}). R²: Correlation coefficient of velocity comparison to linear regression model. RMS: Root mean square error between velocity measurements (m s^{-1}). For all values, error ranges are in parentheses.

Variables	Comment
m_present_time	Unix time.
m_depth	Or use sci_water_pressure * 10 for meters.
m_pitch	In radians.
m_heading	Use heading corrected for compass bias.
m_water_vx, m_water_vy	Water velocities required for using current correction.
m_vx_lmc, m_vy_lmc	Glider horizontal velocity in Local Mission Coordinates
m_speed	Dampened glider horizontal speed.
m_x_lmc, m_y_lmc	Glider position. Requires “x_dr_state” to identify whether position is based on calculation or GPS positioning. Recalculate for with heading correction.
x_dr_state	Identifies glider status.
m_dr_fix_time	Duration of glider on surface without GPS positions. May need to recalculate.
m_dr_postfix_time	Duration of glider on surface with GPS positions. May need to recalculate.
m_gps_x_lmc, m_gps_y_lmc	Glider GPS position in Local Mission Coordinates.
m_dr_surf_x_lmc, m_dr_surf_y_lmc	Glider estimated surface position in Local Mission Coordinates. The variable must be recalculated.
m_dr_time	Duration of glider dive. May need to recalculate.

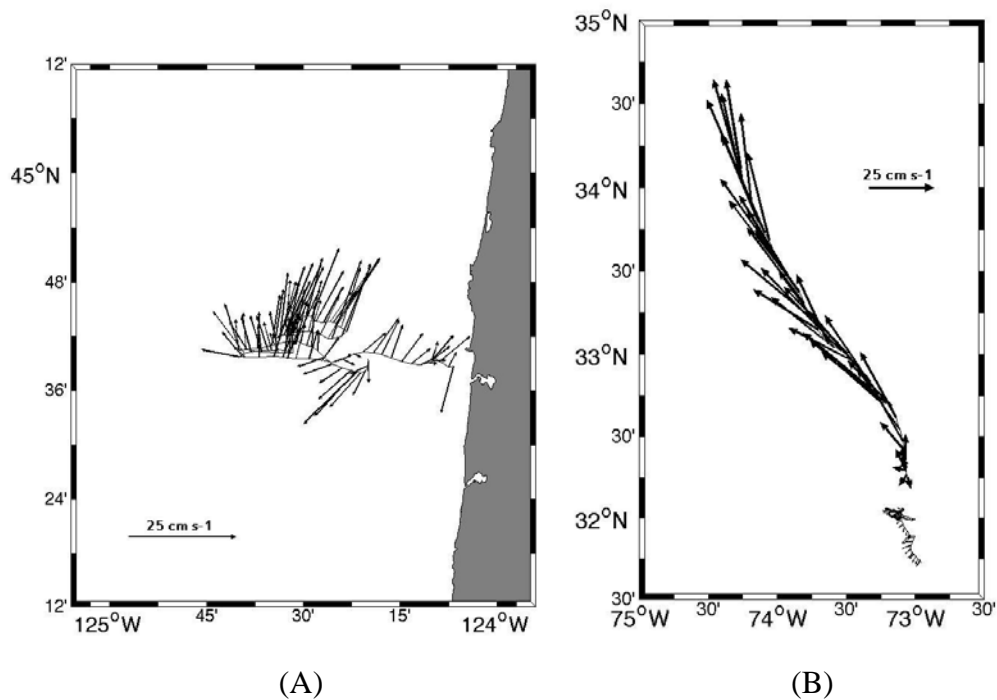
TABLE 2.3: Minimum TWR Slocum variables required to re-calculate dive-average current velocity.



(A)

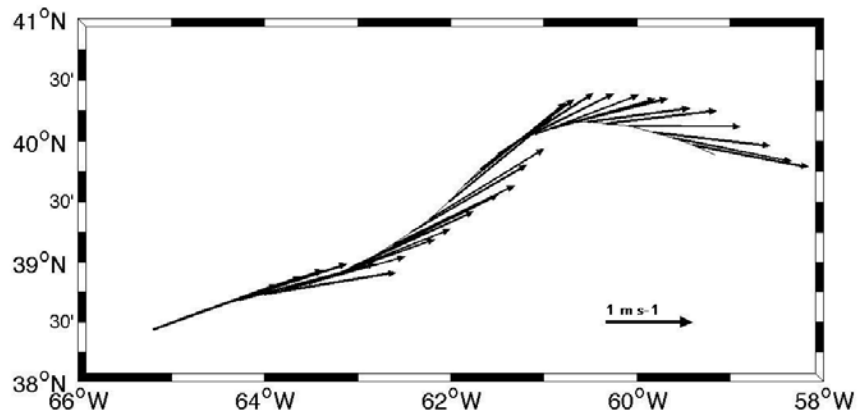
(B)

FIGURE 2.1: ADCP Glider Photographs. (A): ADCP glider. (B): ADCP Phased Array transducer and bio-optic sensors on bottom of glider.



(A)

(B)



(C)

FIGURE 2.2: Map of Glider Deployments and Dive-Average Currents. (A) Oregon coast deployment. (B) Sargasso Sea deployment. (C) Gulf Stream deployment.

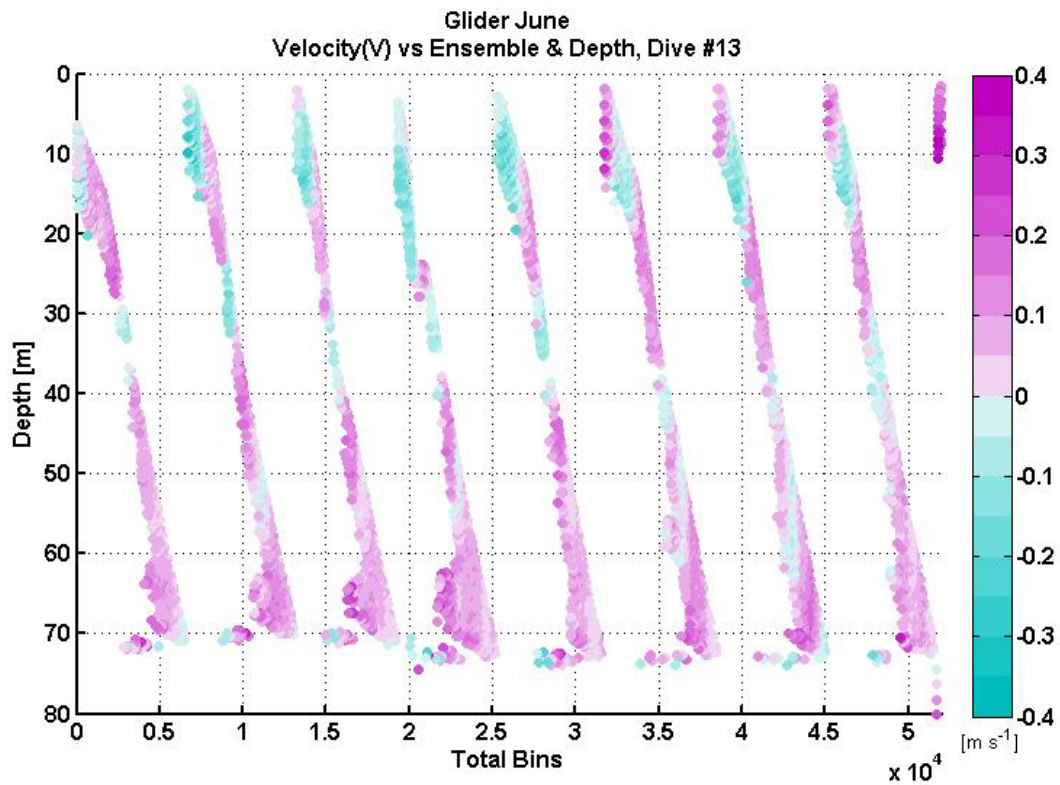


FIGURE 2.3: Raw velocity measurements vs. depth and all bins for Dive #13 of Oregon Coast deployment.

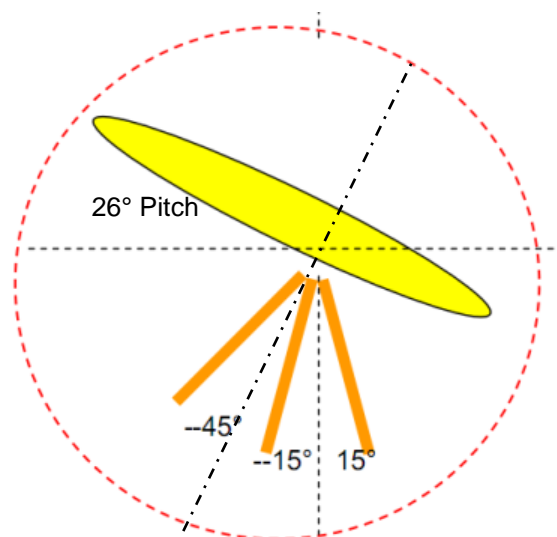
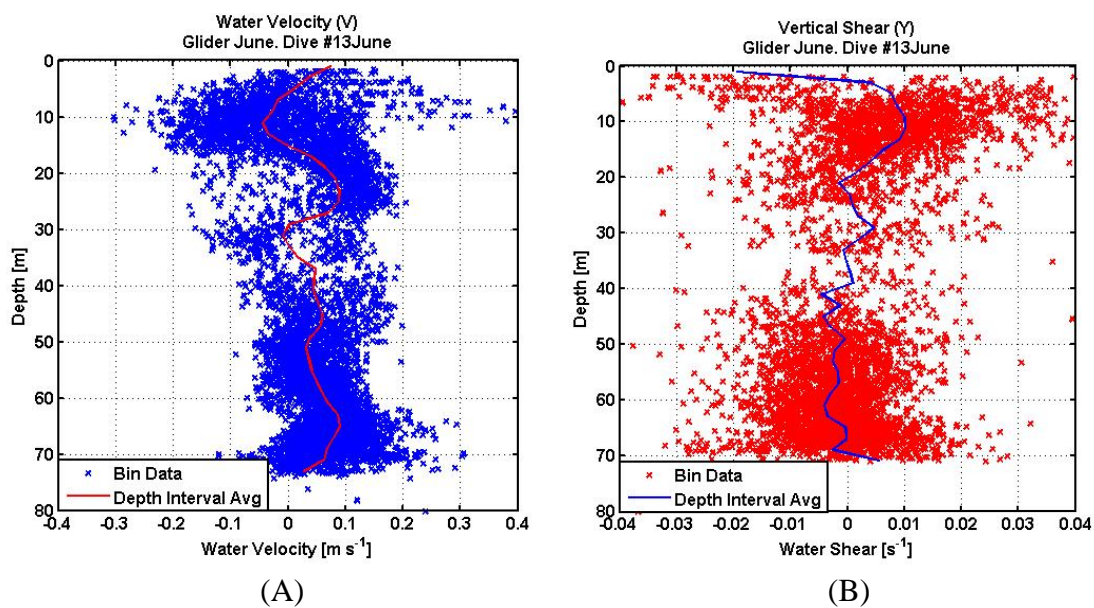
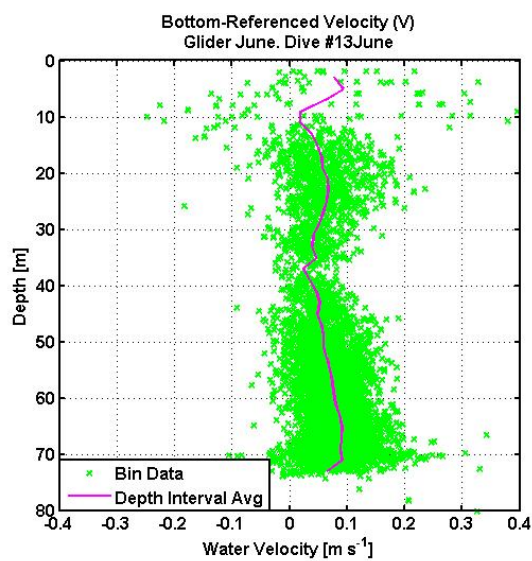


FIGURE 2.4: Mounting Arrangement Beam Angles of Glider-Mounted ADCP (Teledyne Webb Research, 2011)





(C)

FIGURE 2.5: Velocity Data and Shear Data Profiles, north direction for Oregon coast dive #13. (A) Raw Velocity. (B) Vertical Shear. (C) Bottom-referenced Velocity.

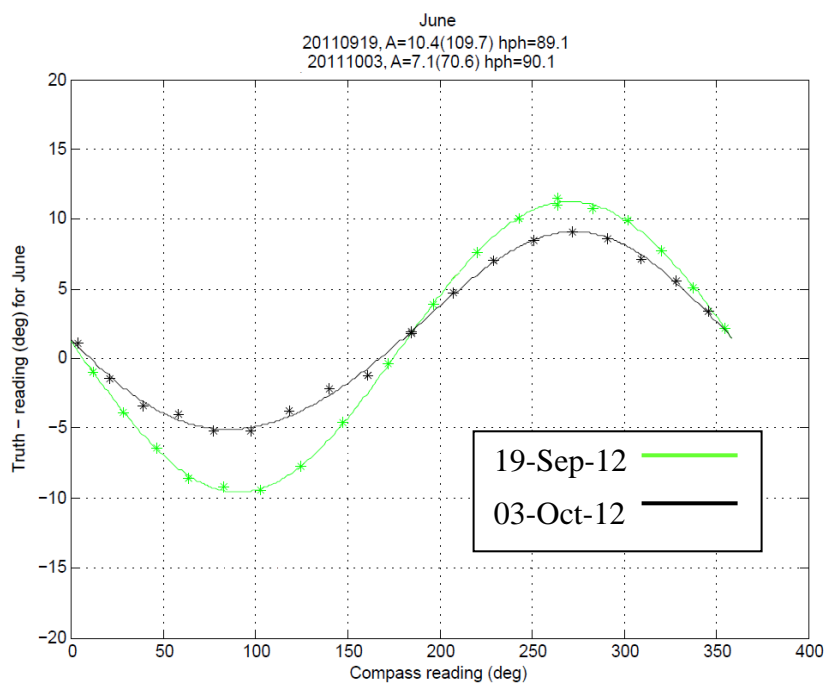


FIGURE 2.6: Compass Correction Curve: Glider June with same battery pack before and after Oregon coast deployment.

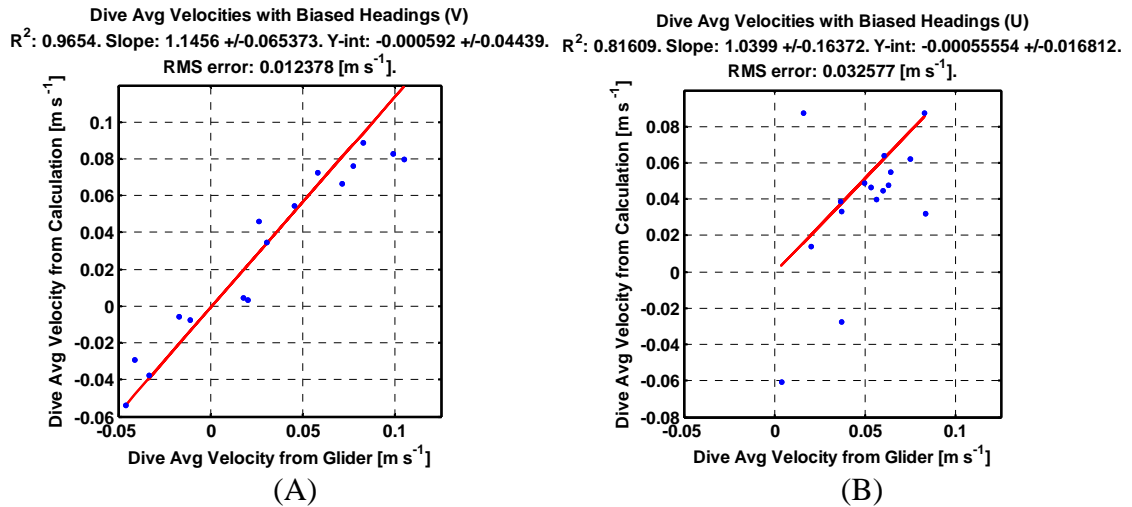


FIGURE 2.7: Regression Plots: Dive-Average Velocities with Biased Headings, Oregon coast dives #2-17. (A) North Velocity, V. Slope: 1.15 ± 0.07 , Y-intercept: $0.00 \pm 0.04 \text{ m s}^{-1}$, $R^2: 0.97$, RMS error: 0.01 m s^{-1} . (B) East Velocity, U. Slope: 1.04 ± 0.16 , Y-intercept: 0.00 ± 0.02 , $R^2: 0.82$, RMS error: 0.03 .

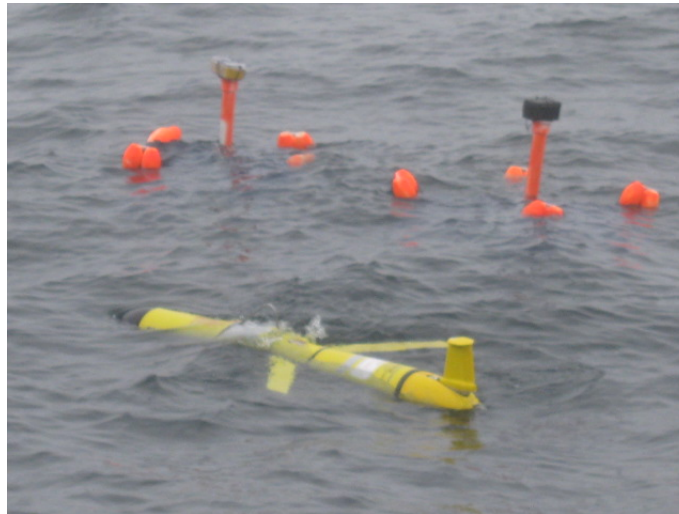


FIGURE 2.8: Photograph of Glider Drift Test.

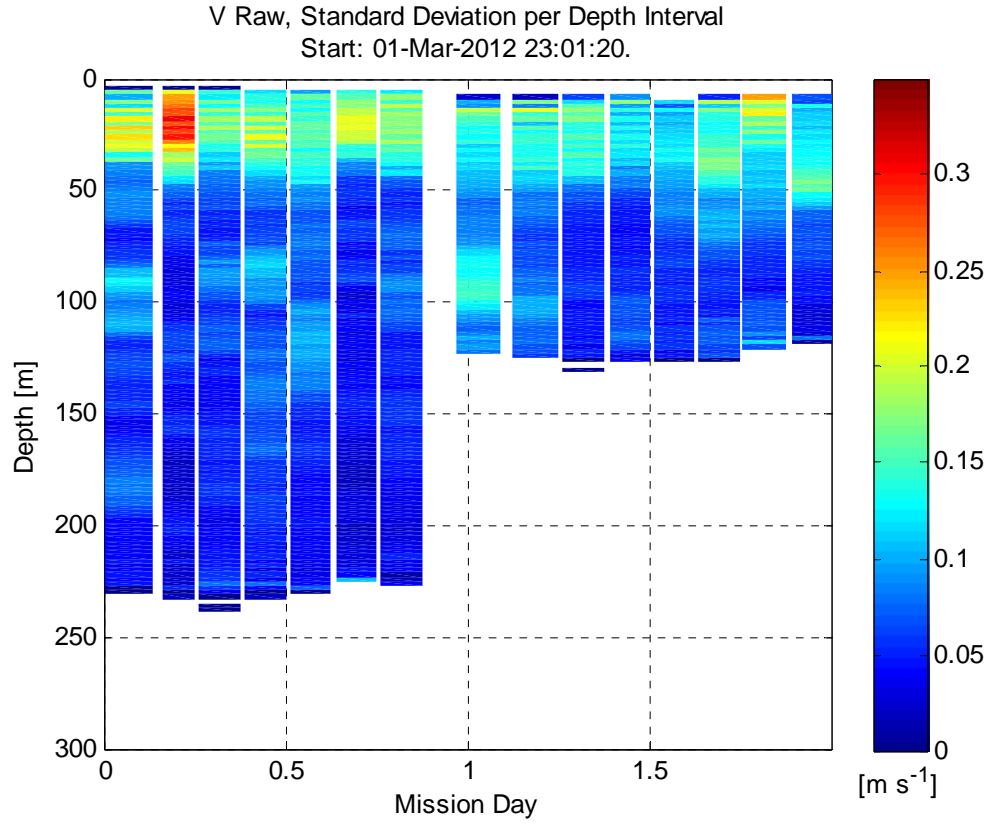


FIGURE 2.9: North velocity depth interval standard deviation.

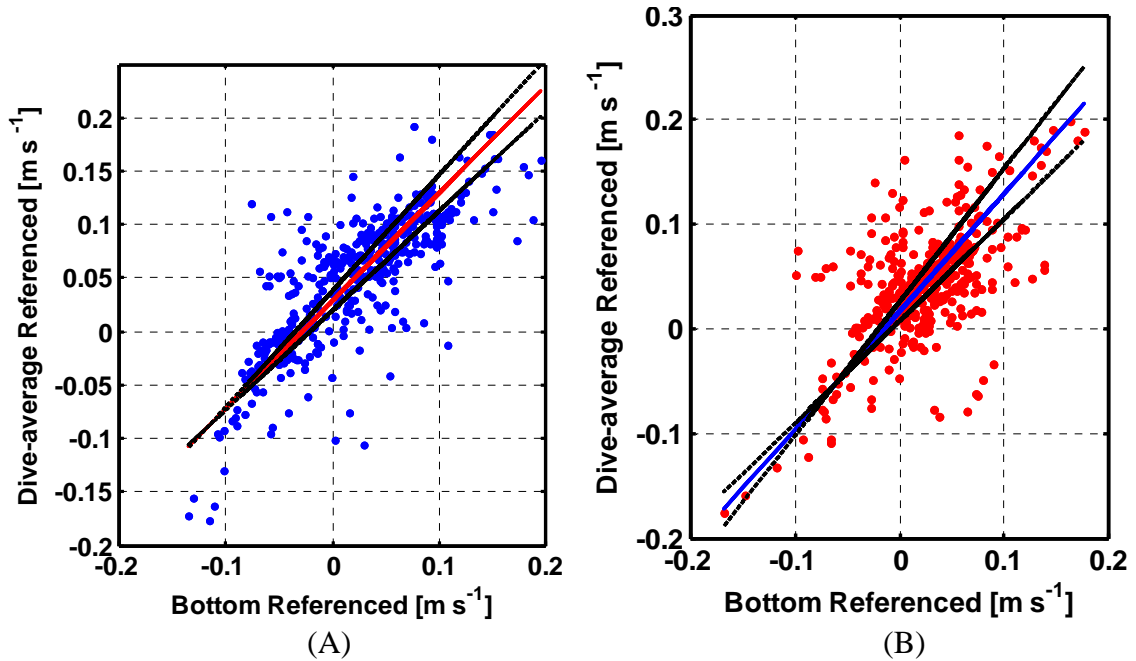


FIGURE 2.10: Oregon Shelf Dives #2-17, Regression Plots: Dive-Average Referenced vs. Bottom-Referenced Depth Interval Velocities. (A) North Velocity, V. (B) East Velocity, U.

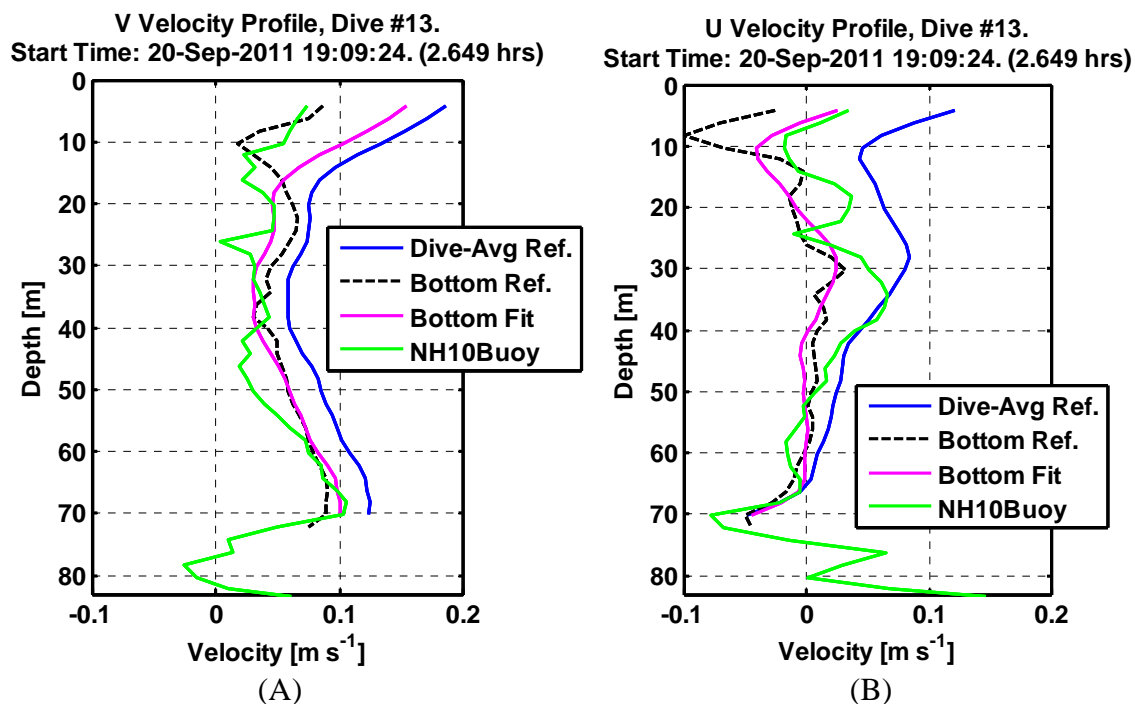


FIGURE 2.11: Oregon Shelf Dive #13: Velocity Profiles

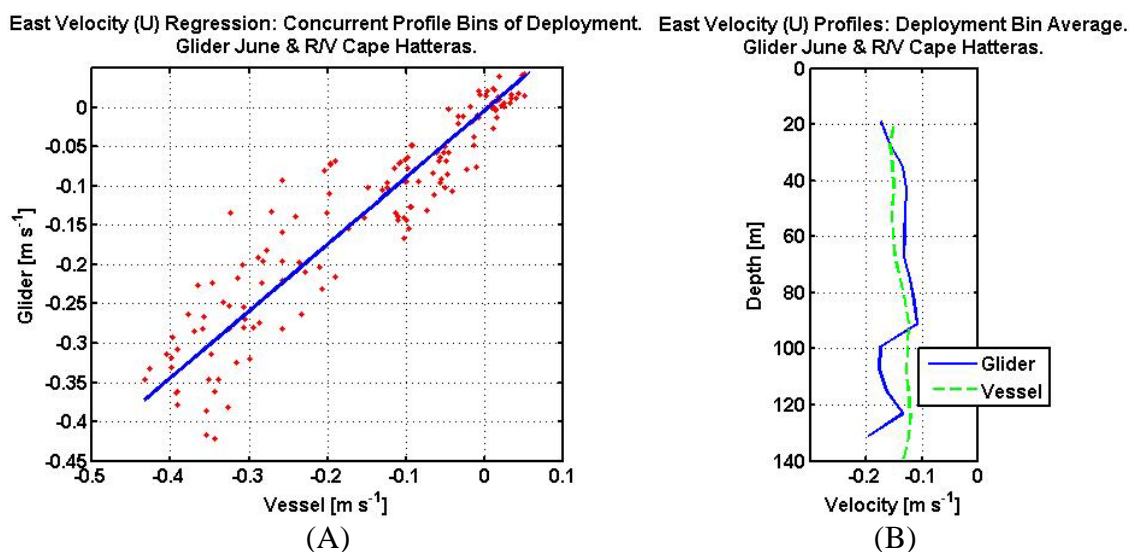


FIGURE 2.12: Cape Hatteras and Glider June Deployment Comparison. (A) Linear regression plot comparing velocities from all concurrent profile bins. (B) Velocity profile bin-average for all concurrent profiles.

3 FURTHER WORK

The results of this research indicates that the modified shear method correctly establishes absolute velocity profiles from the relative velocity measurements of glider-mounted ADCPs. Refinements to this method can increase the velocity accuracy. Alternatively, the inverse velocity solution may be applied to relative glider-ADCP velocity measurements with additional referencing constraints and error mitigation. Advancements in glider-ADCP research may improve incrementally during these initial years of utilization.

This research suggests specific refinements that should be initially investigated. Developing a model of compass bias as a function of battery voltage and based on compass correlation measurements before and after deployments with the same battery pack will increase the accuracy of earth-referenced vector components and dead-reckoning calculations. Experiments depleting the battery pack will be required as the change in compass bias parameters may not be linear with battery pack depletion. Currently, the compass correction is a function of heading with constant parameters derived from one correlation measurement before or after the deployment. Further refinements to the glider dead reckoning and dive-average water current calculations using corrected headings should also be pursued. The calculations used in this research utilize glider dive state parameters but lack the complexity of the Teledyne Webb Research (TWR) proprietary algorithm and could more accurately mimic the TWR calculation. Finding methods to decrease bias in compass measurements sensor may significantly mitigate the inaccuracies associated with compass errors, but will not

entirely eliminate the problem because of the variability of battery pack magnetic influence over the duration of the deployment.

Implementing different operational practices may serve to improve velocity profile accuracy. In seas with highly variable currents (e.g. nearshore), limiting the duration of glider dives may reduce the smoothing effect of the dive-average current calculation. For instance, if the glider encounters an alongshore, surface jet which affects one hour of a three hour dive, the movement of the glider by the jet will influence the horizontal and vertical extents of one profile. Conversely, the dive-average water current calculations from three one-hour dives would spatially refine the jet influence into three absolute velocity profiles during referencing. Similarly, users of high-endurance, high-depth rated gliders (e.g. the 1000-m Slocum Glider with lithium batteries) may record water velocities less frequent than every down-yo to reduce power consumption during extended deployments. If the glider records velocities only during the first 1000m yo, but does not surface until performing several more yos, the dive-average water current will be biased to the dive duration where no ADCP measurements are made. Referencing this dive-average velocity to the relative ADCP measurements may introduce inaccuracies. Surfacing after one yo will limit the bias of non-ADCP measurement flight to one up-yo.

Identifying other sources of measurement bias may reveal errors that require additional mitigations. Previous research has established possible across-ship bias in AUV-mounted ADCPs (Fong and Jones, 2006). Deploying an ADCP glider to fly multiple constant-heading transects of differing orientations in proximity to a stationary and independent ADCP sensor would help establish measurement biases which may or may not be unrelated to compass inaccuracies.

Applying the inverse velocity solution to LADCP measurements has been shown to increase accuracy compared to the shear method when multiple referencing constraints are applied (Thurnherr, 2010). The inverse velocity solution may also be applied to glider ADCP measurements but additional efforts are required to establish low-error referencing constraints. Bottom-track referenced velocities may be referenced to ADCP measurements within range of the seafloor in a similar manner to LADCP research. Whereas LADCP profiles may utilize vessel ADCP measurements as a referencing constrain for upper water column velocities, glider ADCP measurements may reference properly characterized surface drift velocities. In order to utilize surface drift velocities further comparative surface drift experimentation is required to establish possible scaling factors relating glider drift to actual surface currents. Also, as glider ADCP profiles begin beneath the surface, the relation between the surface drift velocity and the upper depth interval of the velocity profile requires proper characterization. The present status of surface drift to top bin velocity characterization in this research indicates limited correlation consistency. Further experimentation and application of fluid dynamic theory may provide a method to better correlate the measurements. For all inverse velocity reference constraints, error sources should be mitigated as much as possible (Thurnherr, 2010).

This research provides an effective method to obtain absolute velocity observations with glider ADCPs. Further research may enable observations with increased accuracy and vertical resolution. Producing absolute velocity profiles from glider ADCP measurements based on depth interval averaging and proper referencing

enables observations based on this technology for use by oceanographic researchers with continued refinements as research progresses.

BIBLIOGRAPHY

Davis, R. E., 1985: Drifter Observations of Coastal Surface Currents During CODE: The Method and Descriptive View. *J. Geophys. Res.*, **90**, 4741-4755.

Davis, R. E., 2010: On the coastal-upwelling overturning cell. *Journal of Marine Research*, **68**, no 3-4, 369-385.

Davis, R. E., C.C. Eriksen and C. P. Jones, 2002: Autonomous Buoyancy-Driven Underwater Gliders. *Technology and Applications of Autonomous Underwater Vehicles*, G. Griffiths, Ed., Taylor and Francis, 37-58.

Fischer, J., and A. M. Visbeck, 1993: Deep Velocity Profiling with Self-contained ADCPs. *J. Atmos. Oceanic Technol.*, **10**, 764-773.

Fong, D. A., and N. L. Jones, 2006: Evaluation of AUV-based ADCP measurements. *Limnol. Oceanogr.: Methods*, **4**, 58-67.

Gourdeau, L., W. S. Kessler, R. E. Davis, J. Sherman, C. Maes, E. Kestenare, 2008: Zonal Jets Entering the Coral Sea. *J. Phys. Oceanogr.*, **38**, 715-725.

Grantham, B. A., F. Chan, K. J. Nielsen, D. S. Fox, J. A. Barth, A. Huyer, J. Lubchenco, B. A. Menge, 2004: Upwelling-driven nearshore hypoxia signals ecosystem and oceanographic changes in the northeast Pacific, *Nature*, **429**, 749-754.

Hickey, B. M., 1998: Coastal Oceanography of Western North America from the tip of Baja California to Vancouver Island. *The Sea*, **11**, A. R. Robinson and K. H. Brink, Eds., John Wiley & Sons, Inc, 345-393.

Huyer A., 1990: Shelf Circulation. *The Sea*, **9** (part B), B. Le Mehaute and D. M. Hanes, Eds., John Wiley & Sons, Inc, 423-466.

Lohrmann, A. and S. Nylund, 2008: Pure Coherent Doppler Systems, 2008, *IEEE/OES 9th Working Conference on Current Measurement Technology*. IEEE, 2008.

Marshall, J. and R. A. Plumb, 2008: Atmosphere, oceans, and climate dynamics: an introductory text. Elsevier Academic Press.

Merckelbach, L. M., R. D. Briggs, D. A Smeed, and G. Griffiths, 2008: Current measurements from autonomous underwater gliders. *IEEE Ninth Working Conference on Current Measurement Technology*, 61-67.

National Geophysical Data Center (NGDC) of the National Oceanic and Atmospheric Administration (NOAA), *Estimated Value of Magnetic Declination*. Retrieved 2012, from <http://www.ngdc.noaa.gov/geomagmodels/Declination.jsp>

RD Instruments, 1996: Acoustic Doppler Current Profile principles of operation a practical primer, 2ND Ed. [P/N 951-6069-00]

Rudnick, D. L., R. E. Davis, C. C. Eriksen, D. M. Fratantoni, and M. J. Peery, 2004: Underwater Gliders for Ocean Research. *Marine Technology Society Journal*, **38**, no. 1, 48-59.

Schofield, O., J. Kohut, D. Aragon, L. Creed, J. Graver, C. Haldeman, J. Kerfoot, H. Roarty, C. Jones, D. Webb, and S. Glenn, S. 2007: Slocum Gliders: Robust and ready. *J. Field Robotics*, **24**, 473–485.

Teledyne RD Instruments, Inc., 2010: Explorer DVL Operation Manual. [P/N 95B-6027-00]

Teledyne Webb Research, 2011: RDI ADCP Sensor Glider Integration Revision 01 [Draft]

Teledyne Webb Research, 2009: User Manual, Slocum Glider Version 02. East Falmouth, Massachusetts, USA.

Thurnherr, A. M., 2010: A Practical Assessment of the Errors Associated with Full-Depth LADCP Profiles Obtained Using Teledyne RDI Workhorse Acoustic Doppler Current Profilers. *J. Atmos. Oceanic Technol.*, **27**, 1215-1227.

Todd, R. E., D. L. Rudnick, M. R. Mazloff, R. E. Davis and B. D. Cornuelle, 2011: Poleward flows in the southern California Current System: Glider observations and numerical simulation. *J. Geophys. Res.*, **116**, 1-16.

Visbeck, M, 2002: Deep Velocity Profiling Using Lowered Acoustic Doppler Current Profilers: Bottom Track and Inverse Solutions. *J. Atmos. Oceanic Technol.*, **19**, 794-807.

Woithe, H. C., D. Boehm, and U. Kremer, 2011: Improving Slocum Glider Dead Reckoning Using a Doppler Velocity Log, *OCEANS 2011*, 1-5 IEEE, 2011.